NERVE STIMULATION

WARREN M. GRILL
Duke University
Durham, North Carolina

1. INTRODUCTION

Electrical stimulation of peripheral nerves is a widespread method to study the form and function of the nervous system and a technique to restore function following disease or injury. The overt effects of electrical stimulation on nervous tissue have been known for over a century, but the theory to explain the effects of extracellular stimulation on neural tissue was only derived after the development of classic electromagnetic field theory, the advent of the core conductor theory of nerve fibers (1), and formulation of cable models of nerve cells (2,3). The fundamental understanding provided by quantitative analysis is required for rational design and interpretation of therapies employing electrical stimulation.

Examples of application of peripheral nerve stimulation include the treatment of pain (4), restoration of motor functions following spinal cord injury or stroke (5,6), and treatment of epilepsy by electrical stimulation of the vagus nerve (7,8). Electrical stimulation of sufficient magnitude will lead to generation and propagation of action potentials from the electrode site. The objective of this chapter is to present the fundamental principles underlying nerve fiber excitation. The focus is on electrical stimulation of peripheral myelinated nerve fibers.

2. STRUCTURE OF PERIPHERAL NERVE

Peripheral nerve fibers constitute both myelinated nerve fibers and unmyelinated fibers, but in this chapter we focus on excitation of myelinated nerve fibers. Myelinated nerve fibers, unmyelinated nerve fibers, and intraneural blood vessels constitute the endoneurium and exist in bundles as individual nerve branches or as fascicles within compound peripheral nerve trunks (Fig. 1a). The endoneurium is a privileged space and maintains a microenvironment, separated from the general circulation by a blood-nerve barrier, appropriate to the function and health of the nerve fibers. Each fascicle is surrounded by a tough layer of tightly packed cells called the perineurium. Finally, the individual fascicles in a compound nerve trunk are held together by a meshwork of connective tissue and fat called the epineurium.

Fascicles are arranged topologically according to their eventual anatomical targets. The anatomical studies of Sunderland showed that, in the more distal sections of a nerve trunk, motor axons are arranged into discrete fascicles that eventually branch from the main trunk to innervate single muscles or small groups of muscles (9). This conclusion has been corroborated by other anatomical studies (10), and recent data support the retention of topography at more proximal levels. Intraneural microstimulation has revealed that sensory fibers remain grouped

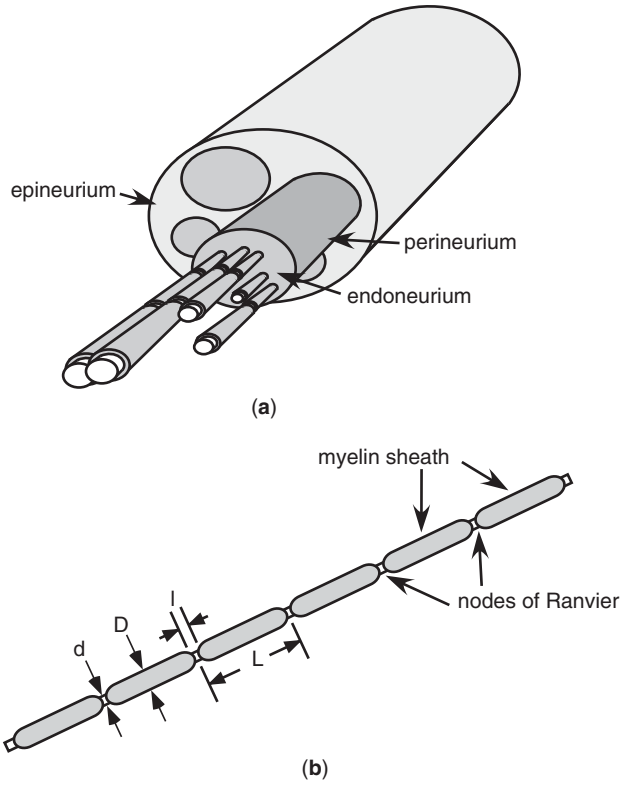

Figure 1. Structure of peripheral nerves. (a) Peripheral nerves are typically composed of multiple fascicles, or bundles of nerve fibers, held together in a matrix of fat and connective tissue called the epineurium. Each fascicle is surrounded by a tight cellular layer called the perineurium that serves to maintain the endoneurial environment around the nerve fibers. (b) The structure of a myelinated nerve fiber consists of a tube of membrane, surrounded over most of its area by the myelin sheath. The myelin sheath is interrupted at regular intervals by exposed sections of membrane called nodes of Ranvier.

even in the more proximal regions of peripheral nerve trunks (11,12), and retrograde staining with horseradish peroxidase has demonstrated that the digital axons within the median nerve of the monkey remain as discrete geometrical groups from the carpal tunnel to the proximal arm (13).

2.1. Nerve Tissue Electrical Properties

Passage of current through tissue generates potentials in the tissue (recall Ohm's Law: $V = IR$). The potentials are dependent on the electrode geometry, the stimulus parameters (current magnitude), and the electrical properties of the tissue. For example, the potential generated by a monopolar point source in a homogeneous, isotropic medium can be determined analytically using the relationship $V_e(r) = \frac{I}{4\pi\sigma r}$, where I is the stimulating current, σ is the conductivity of the tissue medium, and r is the distance between the electrode and the measurement point.

The extracellular potentials are dependent on the electrical properties of the tissue. The electrical properties of peripheral nerves are both inhomogeneous and anisotropic (Table 1) (14–20), and the distribution of potentials within the nerve will depend strongly on the nerve and

electrode geometries. Spatial variations in the electrical properties of the tissue can cause changes in the patterns of activation (21). To calculate the extracellular potentials generated by extracellular stimulation in anisotropic and inhomogeneous tissues requires a numerical solution to Laplace's equation using a discretization method, for example, with the finite element method, (e.g., (22)).

2.2. Nerve Fiber Anatomy

Myelinated nerve fibers are tubes of membrane covered over most of their surface by myelin constituted of Schwann cells (Fig. 1b). The inside of the tubes (intracellular space) includes the axoplasm and intracellular organelles. The myelin sheath around the axon is discontinuous. The internodal regions are covered with myelin and periodic breaks in the myelin sheath expose the underlying membrane at the nodes of Ranvier.

Many of the excitation properties of the nerve fiber (e.g., threshold for excitation, conduction velocity of action potentials) are directly dependent on the morphology of the fiber, and the morphology of the nerve fiber provides the basis for the structure of electrical circuit models of nerve fibers. The diameter of myelinated nerve fibers, D, spans a range of $\sim$1–20 μm and can, to some degree, be correlated with function (Table 2) (23). The geometry of myelinated nerve fibers is quite stereotyped and can be expressed in relation to the fiber diameter (Fig. 1b). In mammals (rat, cat), the internodal spacing, L, is proportional to the fiber diameter ($L = 100^{*}D$), the axon diameter, d, is proportional to the fiber diameter, D, ($d = 0.7^{*}D$), and the nodal length is approximately 1.5 μm (24).

Table 1. Electrical Properties of Peripheral Nerve Tissues

Tissue Type	Electrical Conductivity (S/m)	Reference
Epineurium	0.037	14 (assumed same as fat)
Perineurium	0.0021	15*
Nerve fiber bundles	anisotropic	
Transverse	0.010	16 (toad sciatic nerve)
	0.082	17 (cat dorsal columns)
	0.13	18 (cat internal capsule)
Longitudinal	0.41	16
	0.50	17
	1.2	18
Encapsulation tissue	0.16	19

*The conductivity of perineurium was estimated from *in vitro* measurements of the specific conductance (S/m^2) of perineurium in frog and measurements of the thickness of the perineurium from cat sciatic nerve (30 μm) (20). Measurements of the conductivity of perineurium in mammals have not been conducted.

3. THRESHOLD AND PROPAGATION

A nerve fiber can be stimulated by changing the potential across the nerve fiber membrane (depolarization). At rest, the potential across the membrane is approximately −70 mV, measured inside with respect to outside. Making the transmembrane potential less negative, referred to as depolarization, is required to generate excitation and initiation of an action potential. Following artificial electrical excitation at a certain point along the fiber, the action potential will generally propagate in both directions away from the site of initiation (Fig. 2). The action potential propagating in the normal or orthodromic direction reaches the terminal of the fiber leading to release of neurotransmitter that can impact the postsynaptic cell. For example, at the synapse between a motor nerve fiber and a muscle cell (the neuromuscular junction), acetylcholine is released to cause muscle contraction. The action potential traveling in the opposite direction from normal (antidromic) will propagate to the cell body in the case of efferent (motor) nerve fibers or to the receptor in the case of afferent (sensory) nerve fibers.

Nerve fibers are nonlinear and respond to an electrical stimulus with an all-or-none response. The response of a nerve fiber to a subthreshold and suprathreshold stimulus is shown in Fig. 2. In response to the smaller stimulus, the

Table 2. Classification of Peripheral Myelinated Nerve Fibers in Mammals (23)

Designation	Type	Fiber Diameter	Actuator
Myelinated motor (efferent)	α	9–20 μm	Extrafusal muscle fibers
	β	9–15 μm	Extra- and intrafusal muscle fibers
	γ	2–9 μm	Intrafusal muscle fibers
Myelinated preganglionic (efferent)		1–3 μm	Postganglionic neurons innervating smooth muscle, cardiac muscle
			Sensor
Myelinated sensory (afferent)	Ia	9–22 μm	Primary intrafusal ending
	Ib	9–22 μm	Primary golgi tendon organ ending
	II	5–15 μm	Ruffini endings Secondary intrafusal endings Pacinian corpuscles, hair follicles
	III	1–7 μm	Thermoreceptors, pain fibers

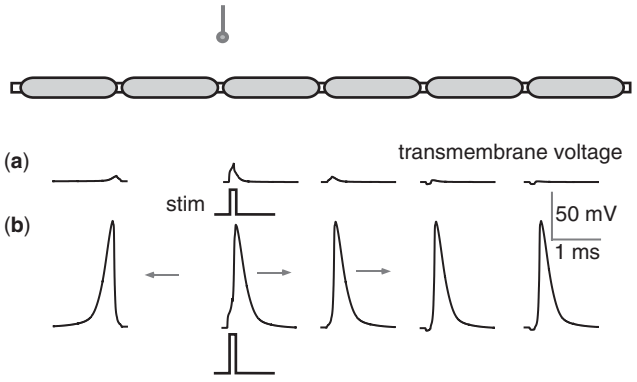

Figure 2. Subthreshold and suprathreshold response of a nerve fiber to an extracellular stimulus pulse. The traces show the transmembrane potential as a function of time in response to stimulus pulse with subthreshold and suprathreshold intensities. (a) The subthreshold stimulus generates a passive response that does not propagate and decays with distance from the node under the electrode. (b) The suprathreshold stimulus generates an action potential that propagates in both directions from the site of initiation.

neural membrane responds in a linear manner, charging and discharging during and after the stimulus, respectively, and no action potential is initiated. When the stimulus is increased above the critical amplitude (threshold), the membrane initiates an action potential as a result of flux of sodium ions from the extracellular space to the intracellular space. This action potential is then propagated in both directions along the fiber.

The velocity at which action potentials travel along myelinated nerve fibers is proportional to the fiber diameter (conduction velocity ≈ 6 m/s per μm of diameter). This relationship develops from the correlation between fiber diameter and internodal spacing ($L = 100D$). As larger diameter fibers have larger internodal spacing, the action potential travels further as it moves from node to node in large diameter fibers than it does in small diameter fibers.

Depolarization of a nerve fiber can be achieved by intracellular current injection resulting in transmembrane current flowing from the intracellular space to the extracellular space or by imposition of an extracellular potential distribution that results in transmembrane current flowing from the intracellular space to the extracellular space. Electrical current pulses delivered through extracellular electrodes located in the vicinity of the nerve fiber can be used to create extracellular potentials in the tissue that, in turn, may lead to the generation of an action potential. The distribution of extracellular potentials is dependent on the electrode geometry, the electrical properties of the extracellular tissue, and the stimulation amplitude, and the effect of the potentials on neurons is dependent on the nerve cell type, its size and geometry, as well as the temporal characteristics of the stimulus.

4. ELECTRICAL CIRCUIT CABLE MODELS OF NERVE FIBERS

Electrical circuits are used to model the electrical behavior of nerve fibers. These circuits, often referred to as core conductor models or cable models, rely on representing the nerve fiber as a series of cylinders (1). Based on the geometry of a nerve fiber (see above), a series of equivalent cylinders are used to represent the fiber geometry. Each cylinder is, in turn, replaced by a "compartment," representing the neuronal membrane, and a resistor representing the intracellular space (25). Thus, the model becomes a series of membrane compartments connected by resistors. Each compartment is itself an electrical circuit that includes a capacitor representing the membrane capacitance of the lipid bilayer, resistors representing the ionic conductances of the transmembrane proteins (ion channels), and batteries representing the differences in potential (Nernst Potential) developing from ionic concentration differences across the membrane. A differential equation describing the electrical potential in the cable as a function of position and time is then solved numerically.

4.1. Models of the Axon

Myelinated axons are composed of continuous tubes of membrane, surrounded at regular intervals by myelin sheaths (Schwann cells), and can be considered as a connection of individual patches of membrane. Each node of Ranvier can be modeled as a membrane patch (25). Adjacent nodes of Ranvier are separated by internodal spaces. If the myelin is assumed to be a perfect insulator, then the internode can be modeled as a tube of axoplasm and represented by an internodal resistance, R_a (Fig. 3). We can calculate the internodal or axoplasmic resistance, R_a, using the internodal spacing, L (recall, $L = 100^*D$, the fiber diameter), and the axon diameter, d (recall, $d = 0.7^*D$).

$$\begin{aligned} R_a &= \text{axoplasmic resistivity}^*\text{internodal length}/ \\ &\quad \text{cross-sectional area of the lumen of the nerve fiber} \\ &= 4^*\rho_a{}^*L/(\pi^*d^2) = 4^*\rho_a{}^*100^*D/(\pi^*(0.7^*D)^2) \\ &= 26\,\text{MΩ}, \end{aligned} \tag{1}$$

for a 10 μm diameter fiber ($D = 10$ μm), with axoplasmic resistivity $\rho_a = 100\,\Omega$ cm.

The individual nodes of Ranvier can be modeled as patches of membrane using a parallel RC circuit (Fig. 3). If we cut and "unroll" each node of Ranvier, then it is straightforward to calculate the values for the membrane resistance, R_m, and membrane capacitance, C_m, from Equations 2 and 3 using the axon diameter, d (recall, $d = 0.7^*D$, the fiber diameter), and the nodal length, $l = 1.5$ μm.

$$\begin{aligned} R_m &= \text{specific membrane resistance}/\text{area of node} \\ &= r_m/\pi^*l^*0.7^*D \\ &= 6063\,\text{MΩ} \end{aligned} \tag{2}$$

for a 10 μm diameter fiber with specific membrane resis-

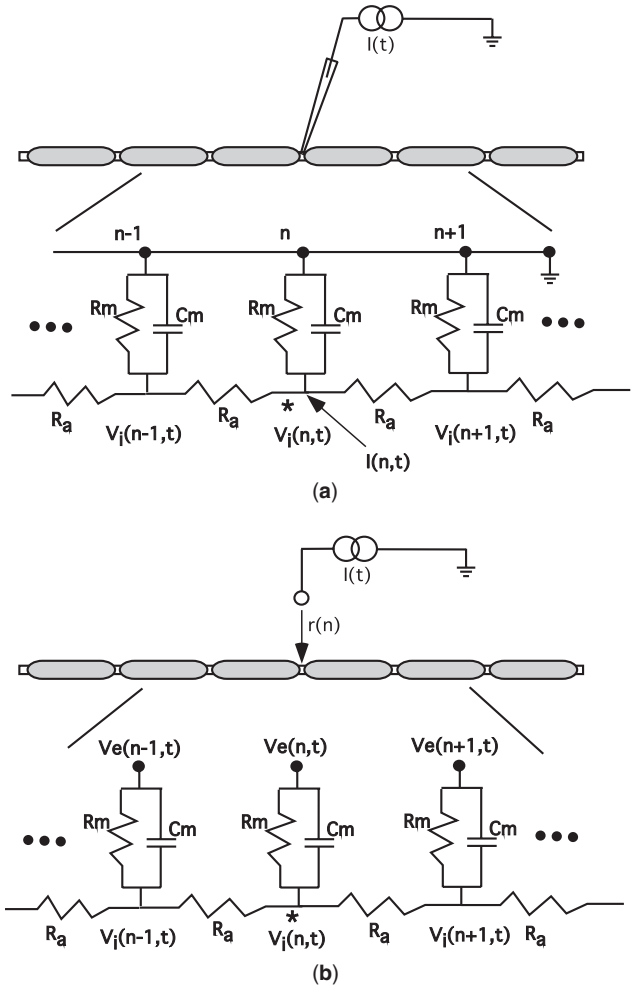

Figure 3. Cable model of a myelinated nerve fiber. (a) Schematic representation of a myelinated nerve fiber in the presence of an intracellular stimulating electrode and the electrical circuit equivalent model. (b) Schematic representation of a myelinated nerve fiber in the presence of an extracellular stimulating electrode and the electrical circuit equivalent model. In the electrical circuit equivalent models, the nodes of Ranvier are represented by the parallel combination of the membrane capacitance, C_m, and the membrane resistance, R_m, and in this simplified representation all membrane conductances are lumped into R_m. Adjacent nodes of Ranvier are connected by resistors, R_a, representing the axoplasm.

tance $r_m = 2000\,\Omega\,\mathrm{cm}^2$.

$$\begin{aligned} C_m &= \text{specific membrane capacitance}^* \text{area of node} \\ &= C_m/\pi^*\mathrm{l}^*0.7^*D \\ &= 0.33\,\mathrm{pF} \end{aligned} \tag{3}$$

for a 10 μm diameter fiber with specific membrane capacitance $C_m = 1\,\mu\mathrm{F/cm}^2$.

4.2. Analytical Descriptions of the Transmembrane Potential

The electrical behavior of the nerve fiber is described by the distribution of the transmembrane potential in time and in space (i.e., along the length of the fiber). In the case of a myelinated nerve fiber, application of Kirchoff's Current Law at node n yields a partial differential (difference) equation for the transmembrane voltage at one node of the fiber (Equation 4), or equivalently, one compartment of the cable model produced by intracellular current injection at one of the nodes of Ranvier (Fig. 3a). Writing Kirchoff's Current Law at node n with positive current defined to enter the node yields

$$\begin{aligned} C_m \frac{dV_m(n,t)}{dt} + \frac{V_m}{R_m} + \frac{[V_m(n-1,t) - 2V_m(n,t) + V_m(n+1,t)]}{R_a} \\ = I(n,t). \end{aligned} \tag{4}$$

This equation is called the cable equation and describes the changes in transmembrane potential generated in a nerve fiber by an intracellular current injection.

Electrical stimulation of peripheral nerve is invariably accomplished with an extracellular current source that generates a set of extracellular potentials outside of the nerve fiber. We now derive an expression for the transmembrane voltage at one node of the fiber (Equation 6), or equivalently, one compartment of the cable model (26). We consider the changes in transmembrane potential produced by an electric field present outside the nerve fiber that sets up potentials at each node of Ranvier, $V_e(n)$. Writing Kirchoff's Current Law at node n (Fig. 3b) yields:

$$\begin{aligned} &\frac{[V_i(n-1,t) - V_i(n,t)]}{R_a} + \frac{[V_i(n+1,t) - V_i(n,t)]}{R_a} \\ &+ \frac{[V_e(n,t) - V_i(n,t)]}{R_m} + C_m \frac{d[V_e(n,t) - V_i(n,t)]}{dt} = 0. \end{aligned} \tag{5}$$

We then apply the definition of reduced transmembrane voltage $V_m(n,t) = V_i - V_e$, and rearrange with the source term on the right side yielding

$$\begin{aligned} &C_m \frac{V_m(n,t)}{dt} + \frac{V_m(n,t)}{R_m} \\ &\quad - \frac{[V_m(n-1,t) - 2V_m(n,t) + V_m(n+1,t)]}{R_a} \\ &\quad = \frac{[V_e(n-1,t) - V_e(n,t) + V_e(n+1,t)]}{R_a}. \end{aligned} \tag{6}$$

This equation is called the cable equation and describes the changes in transmembrane potential generated in a nerve fiber by a set of extracellular potentials.

Examining the right-hand side (source) of the two differential Equations 5 and 6 indicates that an intracellular current source is equivalent to an extracellular source defined by the second spatial difference of the extracellular

potentials.

$$\frac{[V_e(n-1,t) - V_e(n,t) + V_e(n+1,t)]}{R_a} = I(n,t). \qquad (7)$$

Therefore, the response of the nerve fiber to an extracellular field is the same as the response of the fiber to an set of intracellular currents distributed along the length of the fiber, where the magnitude of each current source is defined by Equation 7 (27).

4.3. Spatial Distribution of the Transmembrane Potential

Examples of the distribution of transmembrane potentials generated in myelinated nerve fibers by extracellular stimulation are shown in Fig. 4. The potentials generated in the extracellular space, by passing current through a point source electrode, are shown in Fig. 4a at each node of Ranvier of $D = 4\,\mu m$ and $D = 8\,\mu m$ diameter nerve fibers. The peak extracellular potential occurs outside the node positioned directly under the electrode and is the same in both fibers. However, the change in potential between adjacent nodes is much larger in the 8 μm fiber than in the 4 μm fiber because the nodes are further apart (recall, $L \approx 100^{*}D$). The second difference of the extracellular potentials is the source term that drives membrane polarization (27,28), and thus the same distribution of extracellular potentials gives rise to a larger change in transmembrane potential in the 8 μm fiber than in the 4 μm fiber. This result is seen clearly in Fig. 4b, which illustrates the normalized change in transmembrane potential generated in each of the fibers. The magnitudes of the transmembrane potentials were normalized by dividing by the peak value for the 8 μm fiber to illustrate that the changes in transmembrane potential are larger for the 8-μm diameter nerve fiber. Also, note the triphasic shape of the transmembrane potential distribution along the fibers. The nerve fibers are depolarized immediately beneath the electrode (which is where action potential initiation will occur) and hyperpolarized in regions lateral to the electrode.

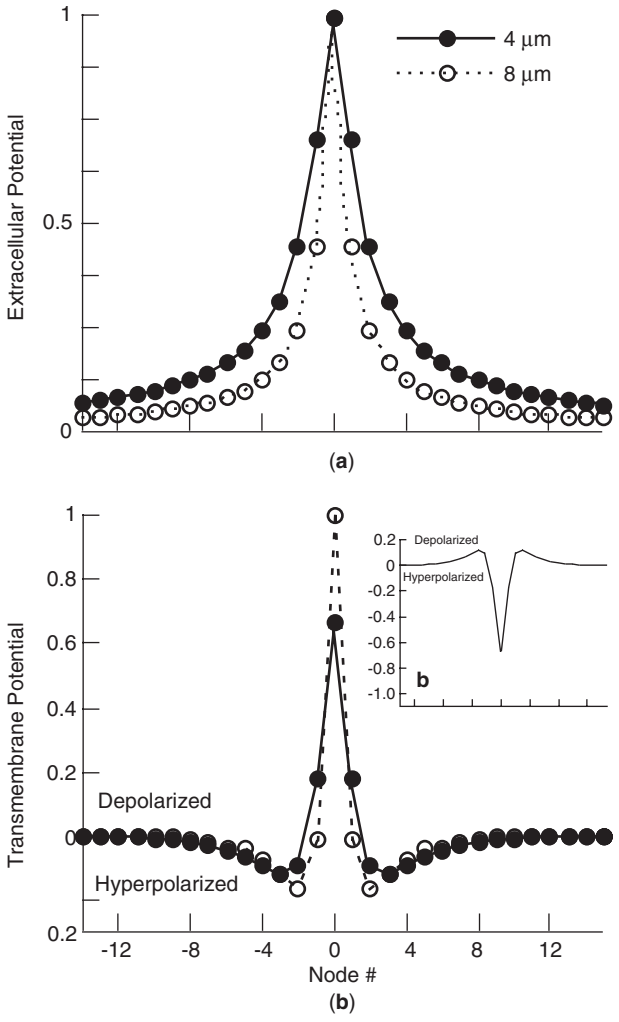

Figure 4. Spatial distribution of the response of myelinated nerve fibers to extracellular stimulation. (a) Normalized extracellular potentials at each node of Ranvier in 4-μm and 8-μm diameter nerve fibers generated a point source electrode positioned 1 mm above the central node of the fibers. The extracellular potential was calculated using $V(r) = I\rho/4\pi r$, where I is the stimulating current (0.1 mA), ρ is the resistivity of the extracellular medium (500 Ω cm), and r is the electrode to node distance. (b) Profile of transmembrane potential generated in the 4 μm and 8 μm nerve fibers. The transmembrane potentials were normalized to the peak value in the 8 μm fiber to illustrate the difference between the two diameters. Maximum depolarization occurs in the node directly under the electrode and is surrounded by flanking regions where the nodes are hyperpolarized. The inset (b) shows the transmembrane potential generated by reversing the stimulus polarity.

5. EXCITATION PROPERTIES OF MYELINATED NERVE FIBERS

In this section, the fundamental factors that govern electrical stimulation of the nervous system are reviewed. An understanding of these relationships is necessary to understand how neural prostheses function and important to the design of safe and effective devices and protocols for functional stimulation.

5.1. Strength-Duration Relationship

The stimulus amplitude necessary for excitation of a single nerve fiber, I_{th}, increases as the duration of the stimulus is decreased. The strength-duration relationship (Equation 8), (29) describes the threshold current required to excite a single fiber as a function of the stimulus pulse duration (PW), and an example of a strength-duration curve is shown in Fig. 5a.

$$I_{th} = I_{rh}[1 + T_{ch}/PW]. \qquad (8)$$

The parameter I_{rh} is the rheobase current and is defined as the current amplitude necessary to excite the neuron with a pulse of infinite duration. The parameter T_{ch} is the chronaxie and is defined as the pulse duration necessary

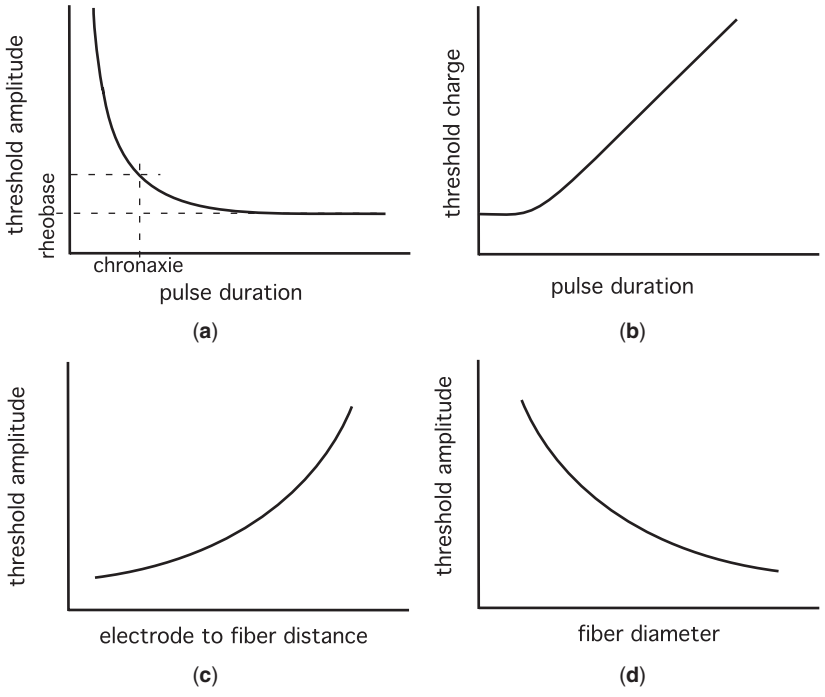

Figure 5. Properties of nerve fiber stimulation. (a) The strength-duration curve of neural excitation relates the stimulation pulse amplitude to the stimulation pulse duration. The rheobase is the stimulation intensity required for excitation with a stimulus pulse of infinite duration, and the chronaxie is the minimum pulse duration required for excitation when the stimulus amplitude is equal to twice the rheobase intensity. (b) The charge-duration curve of neural excitation relates the stimulation pulse charge (amplitude * duration for rectangular pulses) to the stimulation pulse duration. (c) The threshold intensity required for nerve fiber stimulation varies directly with the square of the distance between the electrode and the nerve fiber. (d) The threshold intensity required for nerve fiber stimulation varies inversely with the square root of the diameter of the nerve fiber.

to excite the neuron with a pulse amplitude equal to twice the rheobase current.

5.2. Charge-Duration Relationship

The amount of charge necessary for excitation, Q_{th}, can be determined directly by integration, with respect to time, of the strength-duration relationship. The charge-duration relationship (Equation 9) describes the threshold charge required to excite a single fiber as a function of the stimulus pulse duration (PW), and an example of a charge-duration curve is shown in Fig. 5b.

$$Q_{th} = Q_{rh}[PW + T_{ch}]. \tag{9}$$

The charge required for excitation decreases as the duration of the pulses decreases. Thus, although short pulses require higher currents for excitation, shorter pulses are more efficient at generating excitation than are longer pulses. Reducing the charge required for excitation reduces the probability of electrode corrosion (30) or tissue damage (31) and reduces stimulator power requirements. Shorter pulses also decrease the gain between the stimulus magnitude and the number of nerve fibers activated by increasing the threshold difference between different diameter nerve fibers (32). Similarly, shorter pulses increase the spatial selectivity of stimulation by increasing the threshold difference between nerve fibers lying at different distances from the electrode (33).

5.3. Current-Distance Relationship

The current required for extracellular stimulation of axons also depends on the spatial relationship between the electrode and the nerve fiber and the nerve fiber diameter (26). Transmembrane potentials generated by extracellular current are largest in the fibers closest to the stimulating electrode, thus less current is required to stimulate neurons in the proximity of the electrode. As the distance between the electrode and the fiber, r, increases, the threshold, I_{th}, increases. The change in threshold for excitation of myelinated nerve fibers with distance from a point source electrode is described by Equation 10 called the current-distance relationship.

$$I_{th} = I_R + k \cdot r^2. \tag{10}$$

The offset, I_R, determines the absolute threshold and the slope, k, determines the threshold difference between fibers at different distances from the electrode (34).

5.4. Current-Diameter Relationship

In response to an externally applied stimulus, nerve fibers with a larger spacing between the nodes of Ranvier experience transmembrane potential changes that are larger than those in fibers with a smaller internodal spacing. Under normal conditions, the larger diameter nerve fibers have larger internodal spacings (recall that $L \approx 100^{*}D$). Thus, larger diameters fibers are activated at smaller stimulus amplitudes than the smaller diameter fibers. The dependence of threshold for excitation of myelinated nerve fibers with a point source electrode in homogeneous media, as a function of the fiber diameter, is described by Equation 11, and an example of the current-diameter curve is shown in Fig. 5d.

$$I_{th}(D) = I_D + \frac{a}{\sqrt{D}}. \tag{11}$$

The two constants, a and I_D, are determined from empirical data [e.g., (35)].

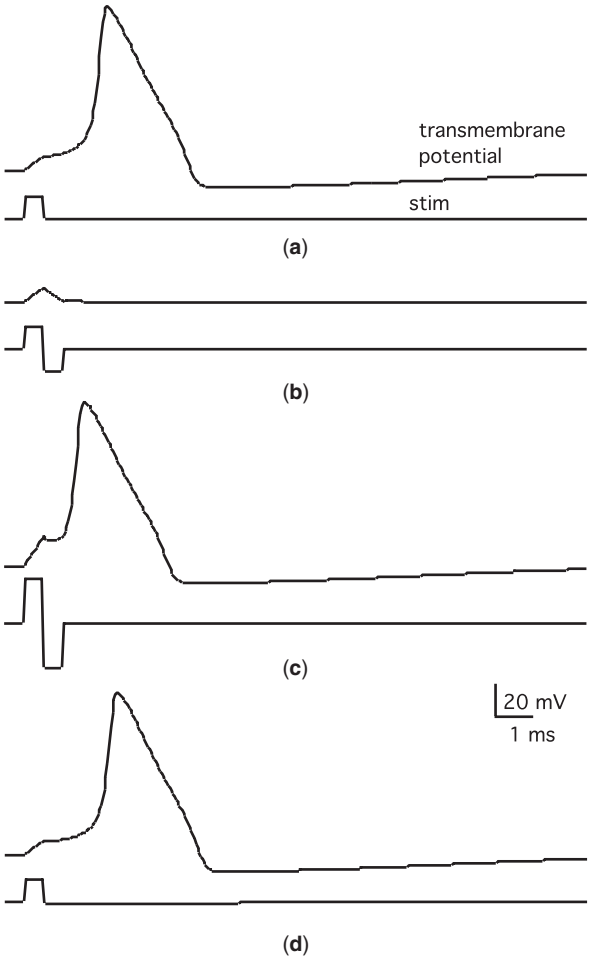

Figure 6. Stimulation of nerve fibers with monophasic and biphasic pulses. Each pair of traces shows the transmembrane potential response to the current stimulus below. (a) Stimulation with a suprathreshold monophasic current pulse generated an action potential (pulse duration (PD) = 0.5 ms, pulse amplitude (PA) = 20 $\mu A/cm^2$). (b) The same stimulus, when followed by a pulse of opposite polarity and equal magnitude, failed to generate an action potential. (c) When the amplitudes of both the first pulse and the second pulse were increased (PD = 0.5 ms, PA = $-40\ \mu A/cm^2$), the biphasic pulse did generate an action potential. (d) Alternatively, if the duration of the second pulse was increased by a factor of ten (PD = 5 ms) and its amplitude was decreased by a factor of ten (PA = $-2\ \mu A/cm^2$), then the original stimulus pulse did generate an action potential. The data were generated using intracellular stimulation in a space-clamped patch of neuronal membrane with Hodgkin–Huxley dynamics (25).

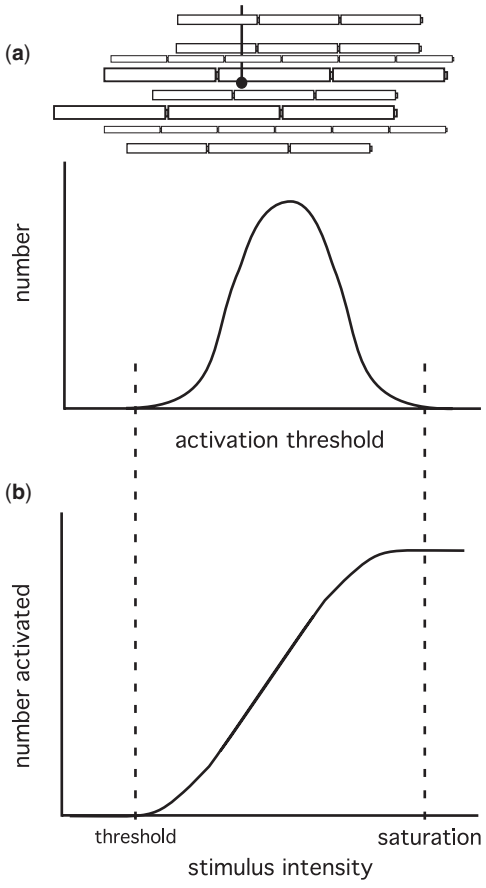

Figure 7. Recruitment of nerve fibers by changes in stimulation intensity. (a) The distribution of nerve fiber diameters and electrode to nerve fiber distances yields a distribution of thresholds to excite individual nerve fibers. (b) The recruitment curve describes the number of nerve fibers stimulated as a function of the stimulus intensity, where the intensity can be modulated through changes in either the amplitude or duration of the stimulus pulse.

5.5. Effects of Stimulus Polarity

The polarity of a monophasic stimulation pulse has a direct influence on the threshold for and pattern of stimulation. Cathodic stimuli applied extracellularly depolarize neuronal membrane in the vicinity of the electrode and an action potential is generated (Fig. 4b). In contrast, anodic stimuli hyperpolarize the membrane immediately adjacent to the electrode. However, anodic stimuli can also generate excitation at the regions of depolarized membrane (called "virtual cathodes") that form adjacent to the region of the neuron hyperpolarized by the stimulus (see inset (b) in Fig. 4b). Action potential initiation will occur at the virtual cathode(s) if the current amplitude is sufficient to bring the depolarized portion of the membrane to threshold. Typically, current thresholds for excitation with an anodal current, via virtual cathodes, are 5–8 times larger than the threshold current for direct cathodal stimulation.

5.6. Monophasic vs. Biphasic Stimuli

Under most conditions, chronic electrical stimulation of the nervous system is accomplished with biphasic stimulus pulses to prevent damage to stimulating electrodes or the underlying tissue (30,36). Although monophasic stimuli are sufficient to generate excitation (Fig. 6a), the second phase of a biphasic stimulus reverses the charge injected by the first phase of the pulse, which may reverse electrochemical reactions at the electrode-electrolyte interface and shift the electrode potential in a direction opposite to that of the primary phase. The second phase of the stimulation waveform, although primarily in place for charge recovery, also has effects on excitation (32,37). The

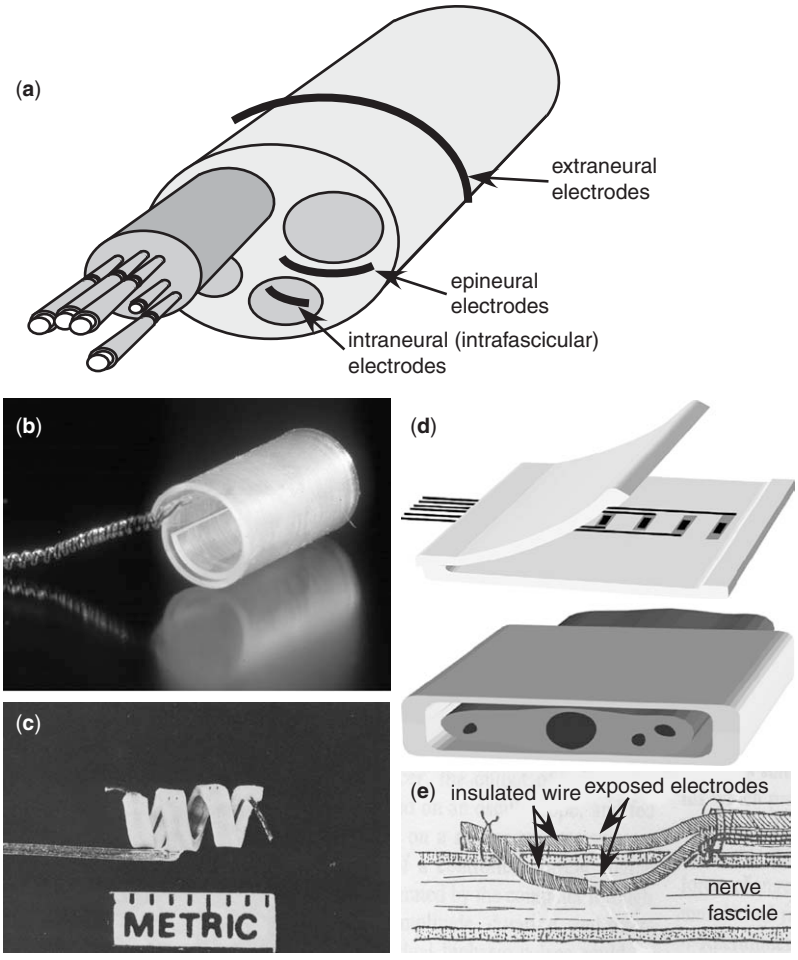

Figure 8. Electrodes for peripheral nerve stimulation. (a) Electrodes for stimulation of peripheral nerve fibers may be placed in (intrafascicular or intraneural electrodes), adjacent to (epineural electrodes), or around a peripheral nerve trunk (extraneural or cuff electrodes). (b) The CWRU spiral nerve-cuff electrode designed to fit snugly around a nerve trunk while enabling expansion and contraction to accommodate changes in nerve diameter (figure courtesy of J. T. Mortimer). (c) The Huntington helix electrode designed to fit snugly around a nerve trunk [figure modified from (40)]. (d) The Flat Interface Nerve Electrode designed to maximize the circumference of the instrumented nerve and afford access to all fascicles for selective stimulation and recording (figures courtesy of P. B. Yoo). (e) Bipolar intrafascicular wire electrodes design to record from or stimulation small groups of nerve fibers [figure modified from (41)].

second phase may arrest an action potential generated by the first pulse and increase the threshold for excitation (Fig. 6b) (25). This effect can be offset by increasing the amplitude of the primary phase (and, in parallel, the amplitude of the secondary phase such that an equal and opposite charge is injected in each phase) or by reducing the amplitude and increasing the duration of the secondary phase (Fig. 6c).

5.7. Recruitment

The stimulation intensity required to activate a single nerve fiber is dependent on the distance between the fiber and the electrode (Fig. 5c) and the diameter of the nerve fiber (Fig. 5d). Thus, the distribution of nerve fiber diameters and electrode to nerve fiber distances within a nerve trunk produces a distribution of thresholds to excite individual nerve fibers (Fig. 7a). The number of nerve fibers stimulated can be regulated through modulation of the stimulation intensity in a process commonly referred to as recruitment. The stimulation intensity can be modulated through changes in either the amplitude or duration of the stimulus pulse (recall the strength-duration relationship, Fig. 5a). The relationship between the stimulus intensity and the number of nerve fibers stimulated is referred to as the recruitment curve (Fig. 7b) (38,39). Increasing stimulus intensity is analogous to cumulative summation (integration) of the distribution of stimulation thresholds, and the cumulative probability distribution describes the number of active nerve fibers as a function of stimulation intensity.

6. ELECTRODES FOR NERVE STIMULATION

Nerve-based electrodes may be placed in, on, or around peripheral nerve trunks (Fig. 8) (40,41), in which locations overcome many of the disadvantages of muscle-based electrodes; however, they also introduce a host of new challenges (39,40). The electrodes may be placed in areas of relatively low stress, minimizing the chances of mechanical failure of the electrodes or leads. Nerve-based electrodes are also unlikely to be subject to length-dependent recruitment properties, as the electrodes do not move relative to the motor nerve fibers (42). Nerve-based electrodes have excitation thresholds that are an order of magnitude lower than those of intramuscular and epimysial electrodes. The use of lower excitation currents permits the use of smaller electrode surfaces to increase selectivity while reducing the risk of electrode or tissue damage.

Nerve-based electrodes also offer the opportunity for more controlled activation of nerve fibers and, thus, more refined control of nervous function. In addition to stimu-

lation, nerve-based electrodes can record afferent activity in peripheral nerves that can be used as a prosthesis command signal or for closed-loop control (43–45). Selective activation of different diameter nerve fibers can be achieved using specialized stimulus waveforms (35,46), and large amplitude depolarizing stimuli can create anodal block of propagation in large nerve fibers at the virtual anodes formed around the central cathode (28,47,48). In addition, small electrodes placed very close to the targeted nerve fibers activate smaller nerve fibers at lower currents than larger nerve fibers (49–51). Similarly, nerve-cuff electrodes can generate unidirectionally propagating action potentials and, thus, block neural transmission via collision block (52).

Nerve-based electrodes also present additional challenges that are not such a concern with muscle-based electrodes. First, because they are in direct contact with neural tissue, nerve-based electrodes may be more likely to cause neural damage than muscle-based electrodes. Selective activation of individual muscles is also more challenging with nerve-based electrodes. Muscle-based electrodes are placed directly in or on the muscles targeted for activation. Although nerve-based electrodes could potentially be placed directly in or on particular nerve branches innervating individual muscles, such an approach makes for a very difficult implant procedure and requires that a separate electrode be placed to activate each targeted muscle.

A number of approaches for selective stimulation of individual muscles with nerve-based electrodes have been developed (53). A successful nerve-based electrode must allow selective and independent control of multiple muscle innervated by a common nerve trunk, it must minimize the potential for damage to the neural tissue, and it must be simple to implant. Selective activation of individual muscles using nerve-based electrodes can be achieved by localizing the region of excitation to specific fascicles or regions of fascicles within a nerve trunk. Thus, an electrode with sufficient spatial selectivity should allow selective activation of an individual muscle without activation of other muscles served by different regions of the same nerve trunk. Nerve-based electrodes thus provide a suitable approach for electrical stimulation of peripheral nerve fibers for restoration of function (5,54).

Acknowledgments

Research in Dr. Grill's laboratory and preparation of this chapter were supported by NIH Grant R21-NS-43450 and R01-NS-050514.

BIBLIOGRAPHY

1. A. L. Hodgkin and W. A. H. Rushton, The electrical constants of a crustacean nerve fiber. *Proc. Royal Soc. B* 1946; **133**:444–479.
2. Lord W.T. Kelvin, On the theory of the electric telegraph. *Proc. Royal Soc.* 1855; **7**:382–399.
3. D. J. Aidley. *The Physiology of Excitable Cells.* Cambridge, MA: Cambridge University Press, 1978.
4. R. L. Weiner, The future of peripheral nerve neurostimulation. *Neurol. Res*. 2000; **22**:299–304.
5. R. B. Stein, P. H. Peckham, and D. P. Popovic, *Neural Prostheses Replacing Motor Function After Disease or Disability.* New York: Oxford University Press, 1992.
6. W. M. Grill and R. F. Kirsch, Neuroprosthetic applications of electrical stimulation. *Assistive Technol.* 2000; **12**:6–20.
7. R. S. Terry, W. B. Tarver, and J. Zabara, The implantable neurocybernetic prosthesis system. *Pacing Clin. Electrophysiol.* 1991; **14**:86–93.
8. The Vagus Nerve Stimulation Study Group, A randomized controlled trial of chronic vagus nerve stimulation for the treatment of medically intractable seizures. *Neurology* 1995; **45**:224–230.
9. S. Sunderland, *Nerves* and *Nerve Injuries*, 2nd ed. New York: Churchill Livingstone, 1978.
10. M. E. Jabaley, W. H. Wallace, and F. R. Heckler, Internal topography of major nerves of the forearm and hand: a current view. *J. Hand. Surg. [Am].* 1980; **5**:1–18.
11. W. Schady, J. L. Ochoa, H. E. Torebjork, and L. S. Chen, Peripheral projections of fascicles in the human median nerve. *Brain* 1983; **106**:745–760.
12. R. G. Hallin, Microneurography in relation to intraneural topography: somatotopic organisation of median nerve fascicles in humans. *J. Neurol. Neurosurg. Psychiatry* 1990; **53**:736–744.
13. T. M. Brushart, Central course of digital axons within the median nerve of Macaca mulatta. *J. Comp. Neurol.* 1991; **311**:197–209.
14. L. A. Geddes and L. E. Baker, The specific resistance of biological material—a compendium of data for the biomedical engineer and physiologist. *Med. Biol. Eng.* 1967; **5**:271–293.
15. A. Weerasuriya, R. A. Spangler, S. I. Rapoport, and R. E. Taylor, AC impedance of the perineurium of the frog sciatic nerve. *Biophys. J.* 1984; **46**:167–174.
16. I. Tasaki, A new measurement of action currents developed by single nodes of Ranvier. *J. Neurophysiol.* 1964; **27**:1199–1206.
17. J. B. Ranck, Jr. and S. L. BeMent, The specific impedance of the dorsal columns of cat: an anisotropic medium. *Exp. Neurol.* 1965; **11**:451–463.
18. P. W. Nicholson, Specific impedance of cerebral white matter. *Exp. Neurol.* 1965; **13**:386–401.
19. W. M. Grill and J. T. Mortimer, Electrical properties of implant encapsulation tissue. *Ann. Biomed. Eng.* 1994; **22**:23–33.
20. W. M. Grill and J. T. Mortimer, Neural and connective tissue response to long-term implantation of multiple contact nerve cuff electrodes. *J. Biomed. Mater. Res.* 2000; **50**:215–226.
21. W. M. Grill, Modeling the effects of electric fields on nerve fibers: influence of tissue electrical properties. *IEEE Trans. Biomed. Eng.* 1999; **46**:918–928.
22. P. H. Veltink, B. K. van Veen, J. J. Struijk, J. Holsheimer, and H. B. Boom, A modeling study of nerve fascicle stimulation. *IEEE Trans. Biomed. Eng.* 1989; **36**:683–692.
23. C.-H. Berthold, Morphology of normal peripheral axons. In: S. G. Waxman, ed., *Physiology and Pathobiology of Axons*. New York: Raven Press, 1978, pp. 3–63.
24. S. G. Waxman, Variations in axonal morphology and their functional significance. In: S. G. Waxman, ed., *Physiology and Pathobiology of Axons*. New York: Raven Press, 1978, pp. 169–190.

25. A. L. Hodgkin and A. F. Huxley, A quantitative description of membrane current and its application to conduction and excitation in nerve. *J. Physiol*. 1952; **117**:500–544.
26. D. R. McNeal, Analysis of a model for excitation of myelinated nerve. *IEEE Trans. Biomed. Eng.* 1976; **23**:329–337.
27. E. N. Warman, W. M. Grill, and D. Durand, Modeling the effects of electric fields on nerve fibers: determination of excitation thresholds. *IEEE Trans. Biomed. Eng*. 1992; **39**:1244–1254.
28. F. Rattay, Analysis of models for extracellular fiber stimulation. *IEEE Trans. Biomed. Eng*. 1989; **36**:676–682.
29. G. Weiss, Sur la possibilite de render comparables entre eux les appareils servant a l'excitation electrique. *Arch. Ital. Biol.* 1901; **35**:413–446. (as cited in H. J. Bostock, *J. Physiol*. 1983; **341**:59–74.)
30. L. S. Robblee and T. L. Rose, Electrochemical guidelines for selection of protocols and electrode materials for neural stimulation. In: W. F. Agnew and D. B. McCreery, eds., *Neural Prostheses: Fundamental Studies*. Englewood Cliffs, NJ: Prentice Hall, 1990, pp. 25–66.
31. D. B. McCreery and W. F. Agnew, Mechanisms of stimulation-induced neural damage and their relation to guidelines for safe stimulation. In: W. F. Agnew and D. B. McCreery, eds., *Neural Prostheses: Fundamental Studies*. Englewood Cliffs, NJ: Prentice Hall, 1990, pp. 297–317.
32. P. H. Gorman and J. T. Mortimer, The effect of stimulus parameters on the recruitment characteristics of direct nerve stimulation. *IEEE Trans. Biomed. Eng.* 1983; **30**:407–414.
33. W. M. Grill and J. T. Mortimer, Effect of stimulus pulse duration on selectivity of neural stimulation. *IEEE Trans. Biomed. Eng.* 1996; **43**:161–166.
34. S. D. Stoney, Jr., W. D. Thompson, and H. Asanuma, Excitation of pyramidal tract cells by intracortical microstimulation: effective extent of stimulating current. *J. Neurophysiol*. 1968; **31**:659–669.
35. Z. -P. Fang and J. T. Mortimer, Selective activation of small motor axons by quasitrapezoidal current pulses. *IEEE Trans. Biomed. Eng.* 1991; **38**:168–174.
36. J. C. Lilly, J. R. Hughes, E. C. Alvord, and T. A. Galkin, Brief noninjurious electric waveform for stimulation of the brain. *Science* 1955; **121**:468–469.
37. C. H. van den Honert and J. T. Mortimer, The response of the myelinated nerve fiber to short duration biphasic stimulating currents. *Ann. Biomed. Eng*. 1979; **7**:117–125.
38. P. E. Crago, P. H. Peckham, and G. B. Thrope, Modulation of muscle force by recruitment during intramuscular stimulation. *IEEE Trans. Biomed. Eng.* 1980; **27**:679–684.
39. D. Popovic, T. Gordon, V. F. Rafuse, and A. Prochazka, Properties of implanted electrodes for functional neuromuscular stimulation. *Ann. Biomed. Eng*. 1991; **19**:303–316.
40. G. G. Naples, J. T. Mortimer, and T. G. H. Yuen, Overview of peripheral nerve electrode design and implantation. In: W. F. Agnew and D. B. McCreery, eds., *Neural Prostheses: Fundamental Studies*. Englewood Cliffs, NJ: Prentice Hall, 1990, pp. 25–66.
41. N. Nannini and K. Horch, Muscle recruitment with intrafascicular electrodes. *IEEE Trans. Biomed. Eng.* 1991; **38**:769–776.
42. W. M. Grill and J. T. Mortimer, Stability of the input-output properties of chronically implanted multiple contact nerve cuff stimulating electrodes. *IEEE Trans. Rehab. Eng.* 1998; **6**:364–373.
43. J. A. Hoffer and M. K. Haugland, Signals from tactile sensors in glabrous skin suitable for restoring motor function in paralyzed humans. In: R. B. Stein, P. H. Peckham, and D. P. Popovic, eds., *Neural Prostheses Replacing Motor Function After Disease or Disability.* New York: Oxford University Press, 1992, pp. 99–128.
44. K. Yoshida and K. Horch, Closed-loop control of ankle position using muscle afferent feedback with functional neuromuscular stimulation. *IEEE Trans. Biomed. Eng*. 1996; **43**:167–176.
45. W. Jensen, S. M. Lawrence, R. R. Riso, and T. Sinkjaer, Effect of initial joint position on nerve-cuff recordings of muscle afferents in rabbits. *IEEE Trans. Neural. Syst. Rehabil. Eng.* 2001; **9**:265–273.
46. W. M. Grill and J. T. Mortimer, Stimulus waveforms for selective neural stimulation. *IEEE Eng. Med. Biol*. 1995; **14**:375–385.
47. I. J. Ungar, J. T. Mortimer, and J. D. Sweeney, Generation of unidirectionally propagating action potentials using a monopolar electrode cuff. *Ann. Biomed. Eng*. 1986; **14**:437–450.
48. C. Tai and D. Jiang, Selective stimulation of smaller fibers in a compound nerve trunk with single cathode by rectangular current pulses. *IEEE Trans. Biomed. Eng.* 1994; **41**:286–291.
49. P. H. Veltink, J. A. Van Alste, and H. B. Boom, Influences of stimulation conditions on recruitment of myelinated nerve fibers: a model study. *IEEE Trans. Biomed. Eng*. 1988; **35**:917–924.
50. W. L. Rutten, H. J. van Wier, and J. H. Put, Sensitivity and selectivity of intraneural stimulation using a silicon electrode array. *IEEE Trans. Biomed. Eng.* 1991; **38**:192–198.
51. A. Branner, R. B. Stein, and R. A. Normann, Selective stimulation of cat sciatic nerve using an array of varying-length microelectrodes. *J. Neurophysiol.* 2001; **85**:1585–1594.
52. C. H. van den Honert and J. T. Mortimer, A technique for collision block of peripheral nerve: frequency dependence. *IEEE Trans. Biomed. Eng*. 1981; **28**:379–382.
53. W. M. Grill, Selective activation of the nervous system for motor system neural prostheses. In: H.-N. L. Teodorescu and L. C. Jain, eds., *Intelligent Systems and Technologies in Rehabilitation Engineering*. Boca Raton, FL: CRC Press, 2001, pp. 211–241.
54. K. W. Horch and G. S. Dillon, *Neuroprosthetics Theory and Practice*. Singapore: World Scientific Publishing, 2004.

FURTHER READING

W. F. Agnew and D. B. McCreery, *Neural Prostheses: Fundamental Studies.* Englewood Cliffs, NJ: Prentice Hall, 1990.

J. K. Chapin and K. A. Moxon, *Neural Prostheses for Restoration of Sensory and Motor Function*. Boca Raton, FL: CRC Press, 2001.

W. E. Finn and P. G. LoPresti, *Handbook of Neuroprosthetic Methods*. Boca Raton, FL: CRC Press, 2003.

F. T. Hambrecht and J. B. Reswick, Electrical stimulation. In: *Functional Electrical Stimulation Applications in Neural Prostheses*. New York: Marcel Dekker, 1977.

K. W. Horch and G. S. Dillon, *Neuroprosthetics Theory and Practice*. Singapore: World Scientific Publishing, 2004.

L. Lou, Uncommon areas of electrical stimulation for pain relief. *Curr. Rev. Pain* 2000; **4**:407–412.

R. B. Stein, P. H. Peckham, and D. P. Popovic, *Neural Prostheses Replacing Motor Function After Disease or Disability.* New York: Oxford University Press, 1992.

H. -N. L. Teodorescu and L. C. Jain, *Intelligent Systems and Technologies in Rehabilitation Engineering*. Boca Raton, FL: CRC Press, 2001.